Journal of Archaeological Science 38 (2011) 1818–1826

Contents lists available at ScienceDirect

Journal of Archaeological Science

journal homepage: http://www.elsevier.com/locate/jas

Optically stimulated luminescence dating of the city wall system of ancient Tayma (NW Saudi Arabia)

Nicole Klasen [a,*], Max Engel [a], Helmut Brückner [a], Arnulf Hausleiter [b], Andrea Intilia [b], Ricardo Eichmann [b], Mohammed H. al-Najem [c], Said F. al-Said [d]

[a] Institute for Geography, University of Cologne, Albertus-Magnus-Platz, D-50923 Köln, Germany
[b] Orient Department, German Archaeological Institute (DAI), Podbielskiallee 69-71, D-14195 Berlin, Germany
[c] Tayma Museum of Archaeology and Ethnography, P.O. Box 22, 71914 Tayma, Kingdom of Saudi Arabia
[d] College of Tourism and Archaeology, King Saud University, P.O. Box 2456, 11451 Riyadh, Saudi Arabia

ARTICLE INFO

Article history:
Received 27 August 2010
Received in revised form
14 March 2011
Accepted 17 March 2011

Keywords:
OSL dating
Geoarchaeology
City wall
Tayma
Saudi Arabia

ABSTRACT

In addition to a series of chronological markers (artefacts, pottery) in the archaeological contexts of ancient Tayma (NW Saudi Arabia), optically stimulated luminescence (OSL) and radiocarbon dating techniques were applied to generate reliable ages for the city wall system of the oasis. A massive aeolian sand deposit burying the oldest part of the outer wall of Tayma was sampled to obtain a minimum age for the construction of this wall. The sequence of OSL ages from the inactive dune (ID) (4900 ± 300 a, 5100 ± 400 a, 4400 ± 300 a, 3900 ± 200 a, 4000 ± 200 a) is in full accordance with ^{14}C-AMS ages of charcoal embedded into the same dune (4190–4420 cal BP, 3870–4080 cal BP). Underlying alluvial samples from the inactive gravel sheet (IGS) in contrast give maximum ages for the construction which scatter between 6600 ± 300 a and 4900 ± 400 a. The new dating sequence provides evidence that the oldest part of the ancient city wall system already existed in the 2nd half of the 3rd mill. BC which is earlier than expected thus far from archaeological and architectural interpretation.

1. Introduction

The oasis of Tayma (NW Saudi Arabia) (Fig. 1) has a rich cultural heritage consisting of a large number of historic buildings and artefacts beginning with the late Neolithic. Throughout antiquity, the site owed its importance to the extensive perennial groundwater resources (Eichmann et al., 2006a). A highly sophisticated system of hydrotechnical installations, probably more than 3000 years old, provided access to water and an efficient use of resources (Hamann et al., 2008).

Archaeological exploration of Tayma started in 1876–78 when Charles M. Doughty discovered and copied several Nabatean inscriptions during his stay (Doughty, 1888), followed by visits of Charles Huber and Jules Euting in 1880 and 1884 (Euting, 1896/1914). Later, systematic surveys and excavations at Tayma were carried out by Philby (1957), Parr et al. (1970), Winnett and Reed (1970), Bawden et al. (1980), Livingstone et al. (1983) and several Saudi archaeologists (e.g., Abu Duruk, 1986; Al-Hajri, 2006; Al-Taimā'i, 2006); for detailed information on the history of the archaeological research at Tayma see Eichmann et al. (2006b, pp. 94–95).

In 2004 the Orient Department of the German Archaeological Institute Berlin (DAI) and the General Commission for Tourism and Antiquities, Kingdom of Saudi Arabia, began a long-term joint project aimed at investigating the culture and the environment of the Tayma oasis and its role within the regional cultural and historical background.

Research activities cover the main ancient settlement mound of Qraya (Fig. 1) as well as the extended city wall system, peripheral burial sites, parts of the ancient water supply system which are distributed over the entire oasis, and also the adjacent sabkha landform, filled by a lake during the early Holocene (Eichmann et al., 2006a, 2006b; Hamann et al., 2008; Hausleiter, 2010; Schneider, 2010; Wellbrock and Grottker, 2010; Engel et al., in press).

Recent investigations extended the chronology of the oasis considerably. Earliest evidence of human activity is represented by Neolithic or post-Neolithic single and multiple flint drills which are attributed to cattle-breeding nomads populating the area during this time. Thus far, data collected from archaeological excavations indicate that the site was settled at least from the Middle Bronze Age (1st half of the 2nd millennium BC) to modern times (Eichmann et al., 2006a). More detailed evidence exists from the Early Iron Age (12th to 9th centuries BC) onwards, when Tayma obtained significant importance as a caravan station at a branch of

* Corresponding author. Tel.: +49 1520 8687029.
E-mail address: nicole.klasen@uni-koeln.de (N. Klasen).

0305-4403/$ – see front matter
doi:10.1016/j.jas.2011.03.018

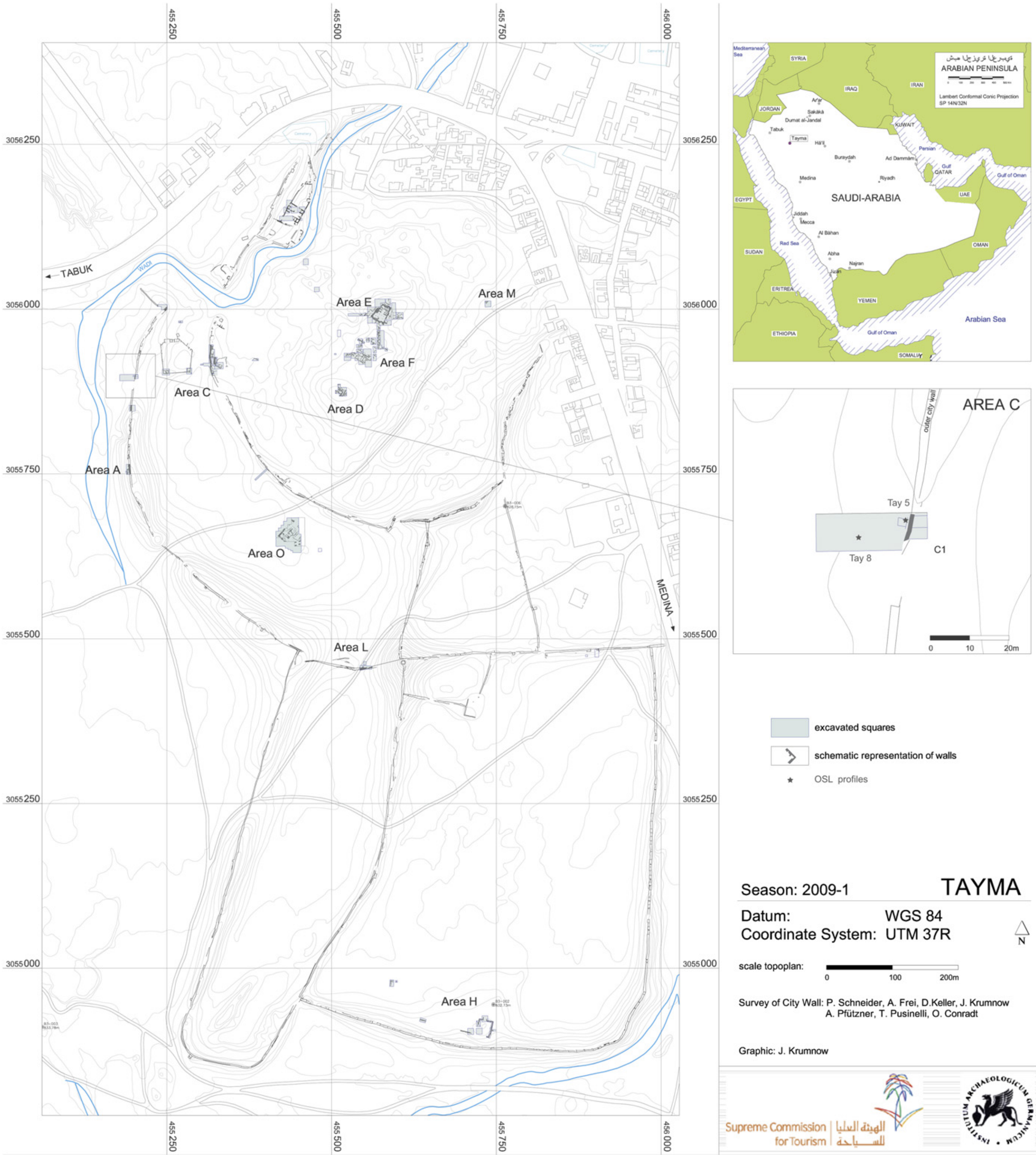

Fig. 1. Site plan of the ancient city of Tayma and the main excavation area (Qraya) indicating excavation square C1.

the so-called Incense Road, linking South Arabia and the Eastern Mediterranean, and because it became the temporary residence of the last Babylonian king Nabonidus (556–539 BC). A clear stratigraphic succession of occupational periods and levels from the Early Iron Age until the Islamic period has been established for the central parts of the site – including numerical dates – whereas the situation of the extended system of walls surrounding the ancient city of Tayma is more complex due to the lack of artefacts and archaeological material directly associated with these constructions. In order to obtain reliable numerical ages for what is apparently the oldest building stage of the city wall system and to integrate these data into the existing chronostratigraphic framework, a systematic approach based on optically stimulated luminescence (OSL) and ^{14}C-AMS dating was implemented. Several OSL

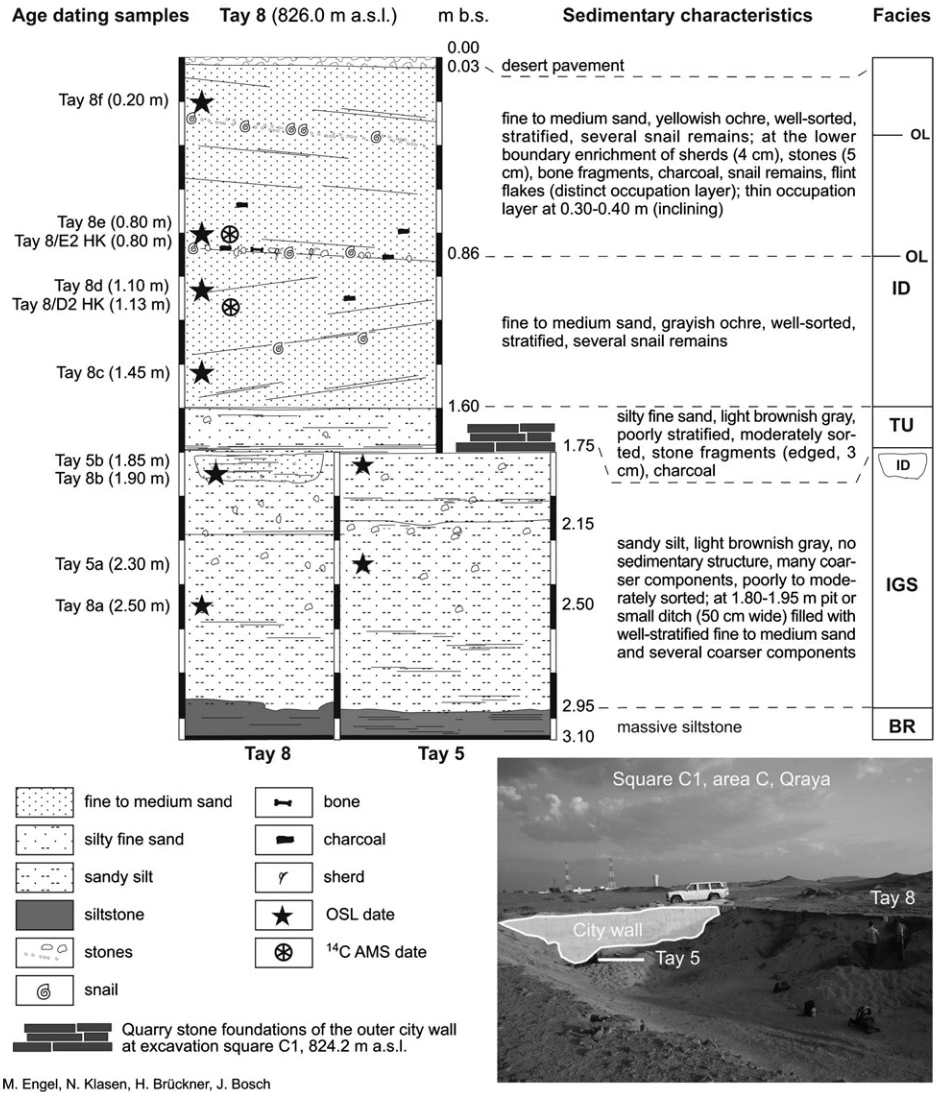

Fig. 2. Sediment profiles Tay 5 and Tay 8 at excavation square C1 (Fig. 2) indicating stratigraphical positions of OSL and ^{14}C samples (ID = inactive dune; OL = occupation layer; TU = transitional unit; IGS = alluvium/inactive gravel sheet; BR = bedrock). The photograph provides an overview of trench C1 outside the outer city wall where the sand burying the construction is partly removed.

studies on Quaternary deposits have been carried out on the Arabian Peninsula (cf. Goudie et al., 2000; Glennie and Singhvi, 2002; Preusser et al., 2002; Bray and Stokes, 2004; Stokes and Bray, 2005; Fuchs et al., 2007; Zander et al., 2007; Blechschmidt et al., 2009; McLaren et al., 2009; Preusser, 2009) and the application of OSL dating in archaeological research is common too (an overview is presented by review articles for example of Feathers, 2003; Wintle, 2008). Anyhow, this paper reports about the first OSL measurements of sediments from Saudi Arabia within the context of archaeological excavations. We present a new dataset of OSL and radiocarbon ages from a dune attached to the outer city wall at the main excavation area of Tayma (referred to as Qraya).

Table 1
Radionuclide concentrations, dose rates, equivalent doses and OSL ages of quartz samples of profiles Tay 5 and Tay 8 (ED: Equivalent dose; D: Dose rate). For aeolian samples the 150–200 μm fraction, for alluvial samples grain sizes of 100–200 μm were chosen. For dose rate calculation, we assumed water contents of 2 ± 1% (aeolian samples) and 4 ± 1% (alluvial samples). Equivalent doses and OSL ages were calculated using the Central Age Model (Galbraith et al., 1999) and ADELE software (Kulig, 2005).

Sample	Lab code	Depth (cm)	U (ppm)	Th (ppm)	K (%)	ED (Gy)	Over-dispersion (%)	D (Gy*ka^{-1})	Age (ka)
Tay 8f	MR0731	20	0.89 ± 0.03	2.90 ± 0.13	0.68 ± 0.01	5.2 ± 0.2	15	1.3 ± 0.1	4.0 ± 0.2
Tay 8e	MR0730	80	1.01 ± 0.03	3.28 ± 0.15	0.47 ± 0.01	4.3 ± 0.1	12	1.1 ± 0.1	3.9 ± 0.2
Tay 8d	MR0729	110	1.64 ± 0.05	4.03 ± 0.18	0.65 ± 0.01	6.5 ± 0.2	15	1.5 ± 0.1	4.4 ± 0.3
Tay 8c	MR0728	145	1.52 ± 0.05	3.44 ± 0.16	0.63 ± 0.01	7.1 ± 0.4	17	1.4 ± 0.1	5.1 ± 0.4
Tay 8b	MR0727	188	2.00 ± 0.07	7.10 ± 0.33	1.70 ± 0.04	13.4 ± 0.4	12	2.7 ± 0.2	4.9 ± 0.3
Tay 8a	MR0826	250	6.70 ± 0.23	12.38 ± 0.57	2.34 ± 0.05	31.22 ± 0.9	14	4.7 ± 0.4	6.6 ± 0.3
Tay 5b	MR0825	185	3.37 ± 0.11	7.41 ± 0.34	1.64 ± 0.03	14.7 ± 1.0	8	3.0 ± 0.4	4.9 ± 0.4
Tay 5a	MR0824	230	5.18 ± 0.18	11.61 ± 0.53	2.27 ± 0.05	25.5 ± 1.2	20	4.2 ± 0.4	6.0 ± 0.4

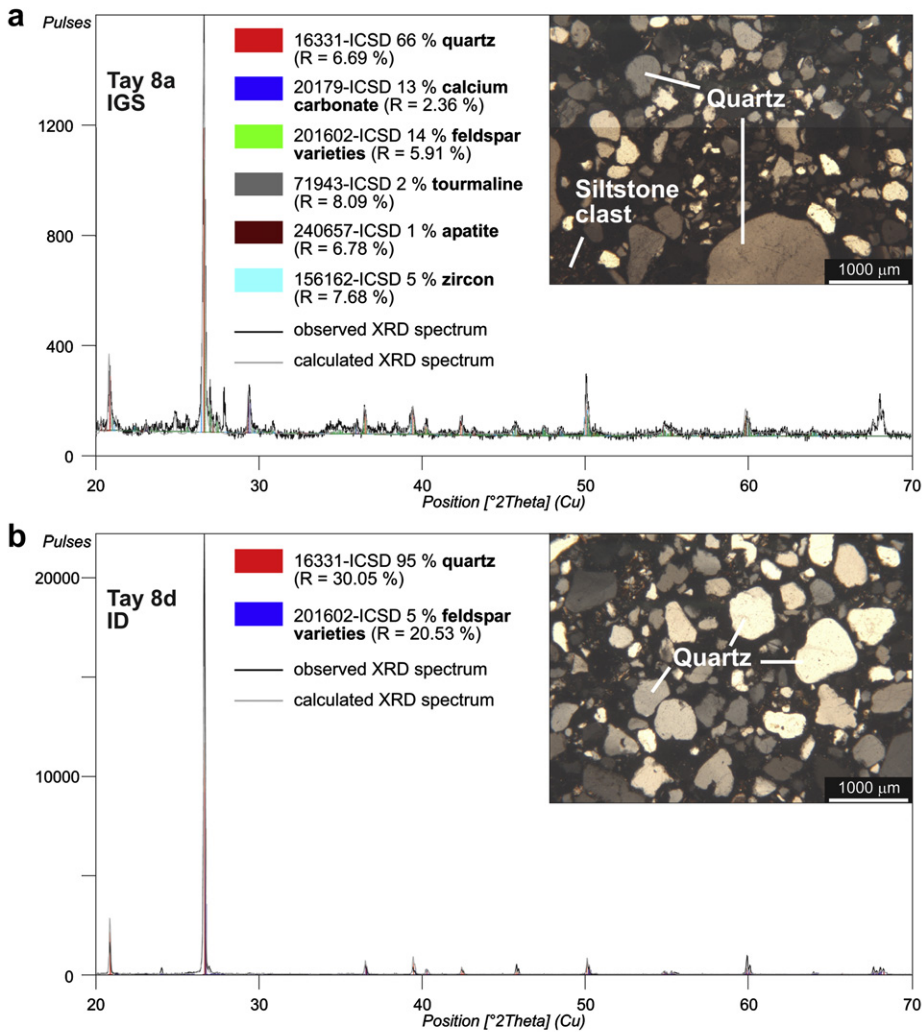

Fig. 3. XRD spectra and thin sections (under crossed nichols) of the aeolian deposit (Fig. 4a) and the underlying alluvium (Fig. 4b). Mineral percentages are based on analyses using the ICSD database, their potential error is indicated by the R value.

This sandy deposit is associated with the existence of the wall – a relationship which has already been recognised during previous archaeological investigations (Intilia, 2010). Therefore, dating its phase of accumulation provides a minimum age for the construction of the wall.

2. The study site

Tayma is located in the southeastern part of the Tabuk province in the arid northwest of Saudi Arabia, more than 800 m above mean sea level (Fig. 1). The area is covered by Palaeozoic sandstone gently dipping northward. Its carbonate cement is severly leached; thus, the loose sand provides a source not only for the An-Nafud erg east of Tayma but also for dune accumulation at obstacles like exposed walls in the urban area and the archaeological excavation. Average rainfall is around 45 mm/a and the prevailing winds blow from the west and northwest. Wind velocities today are relatively low, which is reflected by the occurrence of only few active dunes in the adjacent An-Nafud sand sea (Whitney et al., 1983).

We collected samples for OSL dating from deposits beneath the western outer city wall (profile Tay 5) and from the dune burying the entire construction (profile Tay 8) at excavation square C1 (Fig. 1). Profile Tay 8 is located c. 10 m west of the exposed wall due

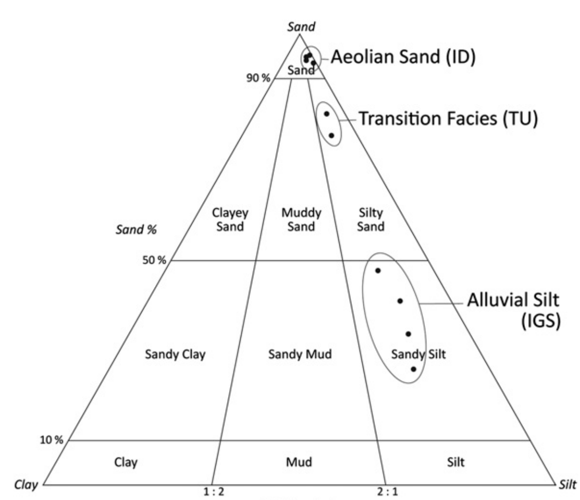

Fig. 4. Triangle diagram reflecting significant differences in mean grain size between the inactive dune (ID) and the inactive gravel sheet (IGS); see also Fig. 3.

Table 2
^{14}C-AMS results (pmC = percent modern [1950 AD] carbon; BP = 1950 AD). Radiocarbon ages were calibrated using Calib 6.0.1 software (Reimer et al., 2009).

Sample	Lab code	Fraction	C weight (mg)	Corr. pmC	^{14}C age (a BP)	δ^{13}C (‰)	cal BP (2σ)	Depth b. surface (cm)
Tay 8/D2 HK	KIA34030	Charcoal, acid residue	2.45	61.72 ± 0.20	3875 ± 25	−24.55 ± 0.43	4190–4420	110–116
Tay 8/E2 HK	KIA34029	Charcoal, humic acid	1.62	63.55 ± 0.22	3640 ± 30	−26.52 ± 0.24	3870–4080	80

to intercalating strata of disintegrated mud-bricks disturbing the stratigraphy of the dune deposit immediately next to the wall (cf. Intilia, 2010).

The wall section at C1 consists of a mud-brick construction on top of a quarry stone foundation, c. 1.1 m wide (Intilia, 2010), and is assumed to be the oldest part of the entire wall system, stretching about 15 km around the oasis. To date, an initial construction age between the late 3rd and the early 2nd millennium BC has been taken into consideration, deduced from flint and carnelian fragments included in the mud-bricks and a ^{14}C age of charcoal remains (Eichmann et al., 2006b; Schneider, 2010; Intilia, 2010), whereas the latest possible date for the upper sandstone construction is the late 2nd millennium BC (Eichmann et al., 2006a).

Sediment profile Tay 5 (Fig. 2) begins with bedrock, a greenish-grey micaceous siltstone of early Ordovician age (Qasim Formation, Hanadir Member). The overlying unit (thickness = 120 cm) represents the substratum of the city wall foundations and consists of unstratified sandy silt with numerous angular rock fragments. Vaslet et al. (1994) refer to this sedimentary unit as alluvium or an inactive gravel sheet (IGS), accumulated predominantly by pre-settlement flooding during more humid phases of the Quaternary. This layer was sampled twice for OSL dating (Tay 5a-b in Table 1).

The IGS unit covers the bedrock over the entire area of Qraya and it can also be traced at profile Tay 8, located about 15 m southwest of Tay 5 (Fig. 2). At the same level where the IGS is vertically confined by the foundations of the city wall at Tay 5, the basal contact of a massive body of aeolian sand was identified at Tay 8. Hence, we conclude that the sand deposit accumulated after the wall had been built. Today the sediment body represents an inactive dune (ID) with a stable desert pavement surface on top and at least two thin fossil occupation layers characterised by an enrichment of charcoal, bone fragments, snail shells and platy angular stones. Between the IGS and the ID we observed an artificial ditch as the earliest evidence of human presence within the stratigraphy. Different sedimentation processes for both sediment units are indicated by X-ray diffraction (XRD) spectra, thin section and grain size analyses. The IGS contains less quartz and higher percentages of feldspar compared to the ID. Calcium carbonate and heavy minerals are even absent in the ID. Thin sections reveal that the ID is only poorly sorted and contains larger polycrystalline siltstone clasts, while in both deposits the grains are moderately rounded (Fig. 3). The ID is significantly coarser (sand) than the underlying IGS (sandy silt) (Fig. 4).

Three samples from the IGS (Tay 8a, Tay 5a, b), one sample from the sandy infill of the ditch (Tay 8b) and four samples from the ID (Tay 8c-f) were taken for OSL dating (Table 1). Additionally, two charcoal fragments were collected from the ID for radiocarbon dating (Tay 8/D2 HK, Tay 8/E2 HK in Table 2).

3. Methodological details

3.1. Sampling and sample preparation

All samples for optically stimulated luminescence dating (OSL) were collected using steel tubes which were emptied into opaque plastic bags. Sample preparation was done under subdued red light conditions to preserve the luminescence signal. First, the samples were dry-sieved and HCl (10%), H_2O_2 (10%) and sodium oxalate were added to remove carbonates, organic material and clay. Sodium polytungstate ($\rho_1 = 2.58$ g cm^{-3}; $\rho_2 = 2.68$ g cm^{-3}) was used to separate coarse grained quartz and hydrofluoric acid (40%, for 40 min) to etch the grains. Finally, the quartz grains were fixed on stainless steel discs with silicon oil in a diameter of 4 mm (aeolian samples) and 2 mm (alluvial samples) per aliquot.

Charcoal samples assigned for ^{14}C-AMS analysis were processed at the ‘Leibniz Labor für Altersbestimmung und Isotopenforschung’, Christian-Albrechts-Universität Kiel (Germany). For calibration purposes, Calib 6.0.1 software (Reimer et al., 2009) was applied. Grain size distributions were investigated by means of the wet

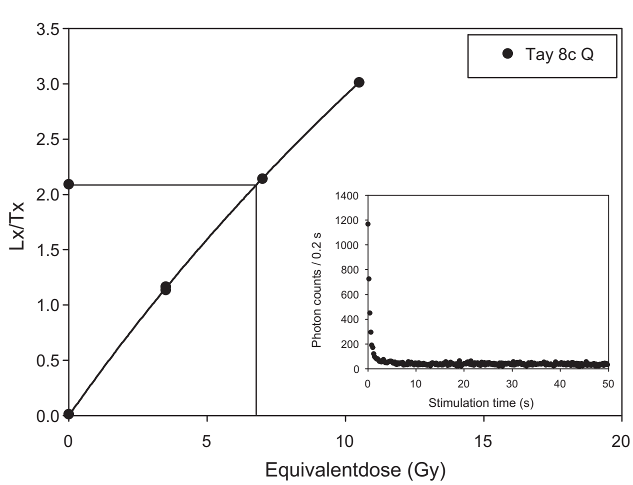

Fig. 5. Dose response curve and decay curve of aeolian quartz sample Tay 8c. The natural luminescence signal is relatively dim regarding the fact that 4 mm aliquots were used.

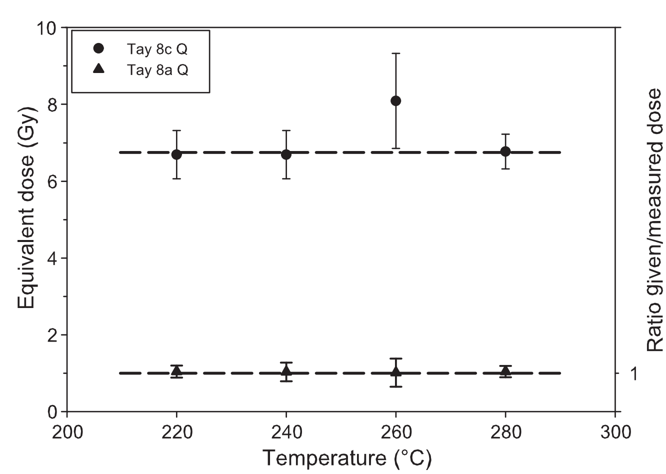

Fig. 6. Preheat plateau test of sample Tay 8c. No preheat temperature dependence on equivalent dose (ED) estimation was reported. Finally, a preheat temperature of 280 °C was chosen for ED determination. For sample Tay 8a, a dose recovery test (DRT) documented the good application of the measurement protocol. The results are given as a ratio of given dose (30 Gy) to measured dose.

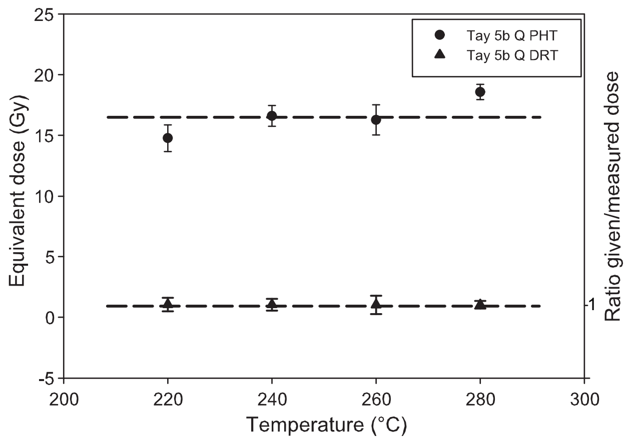

Fig. 7. Preheat plateau test and dose recovery test of sample Tay 5b. A preheat plateau is developed between 240 °C and 260 °C, laboratory doses of 15 Gy were reproduced in a dose recovery preheat plateau test. For further measurements, we chose a preheat temperature of 240 °C for all samples from the alluvial facies.

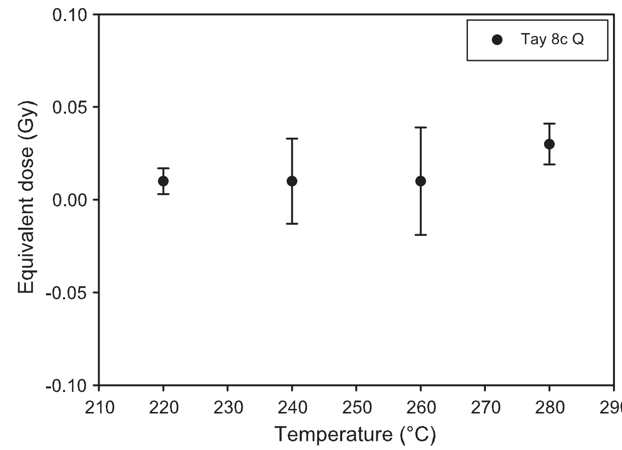

Fig. 9. The unwanted effect of thermal transfer was quantified as reported by Rhodes and Bailey (1997). For aeolian sample Tay 8c, the test showed that thermal transfer did not have any influence on the equivalent dose (ED) estimation of the samples of profile Tay 8.

sieve-pipette technique (Köhn, 1928). Statistical parameters were calculated using Gradistat software (Blott and Pye, 2001). X-ray diffraction (XRD) using a Siemens 5000D powder diffractometer was carried out to document facies differences. The Inorganic Crystal Structure Database (ICSD) was applied to interpret the XRD results.

3.2. Measurement details

OSL measurements were carried out on an automated Risø TL DA 15 reader equipped with a ^{90}Sr/^{90}Y beta source delivering 0.103 Gy/s to the sample. Blue light emitting diodes (470 ± 30 nm) and a Hoya U 340 filter (7.5 mm) transmitting a wavelength of 330 ± 40 nm were used for optical stimulation and signal detection. The dose rate was determined using high resolution gamma-spectrometry. All measurements were carried out with the single aliquot regenerative dose approach (SAR) (cf. Murray and Wintle, 2000). At first, preheat plateau tests and dose recovery tests were performed to examine the applicability of the measurement protocol using preheat temperatures between 220 and 280 °C, a cut heat of 200 °C and OSL stimulation for 50 s at 125 °C. The initial 1 s of the luminescence signal was used and a background of the last 10 s was subtracted to detect the OSL signal (Fig. 5). For dose

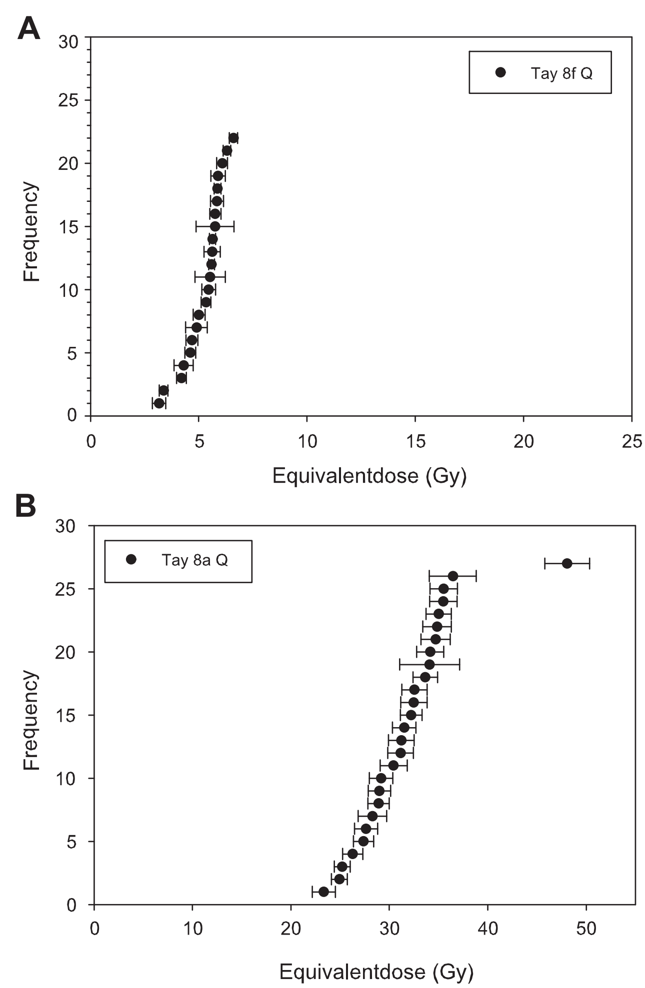

Fig. 10. a) Frequency distribution summarising all aliquots of sample Tay 8f that were used for mean equivalent dose calculation. A lot of aliquots were rejected from the distribution as they did not pass certain criteria, i.e. a luminescence signal that is clearly higher than the background signal or recycling ratios between 0.9 and 1.1. b) Frequency distribution of alluvial sample Tay 8a. The shape is Gaussian with an overdispersion of 14%.

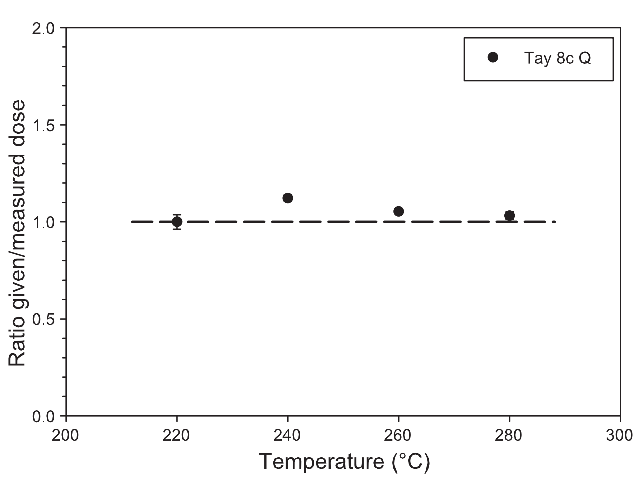

Fig. 8. Dose recovery test carried out on sample Tay 8c. Six aliquots were measured at each temperature level from 220 to 280 °C. A laboratory dose of 6.5 Gy was well reproduced within errors. The results are displayed as given/measured dose ratios.

recovery tests, an artificial dose of 6.5 Gy (aeolian sample Tay 8c), 15 Gy and 30 Gy (alluvial samples Tay 8a, Tay 5b) was applied to the samples after optical bleaching with blue diodes for 200 s.

Mean equivalent doses (ED) were calculated with the Central Age Model (Galbraith et al., 1999) and for dose rate and age calculation ADELE software (Kulig, 2005) was used.

4. Results

No preheat temperature dependence was found for any samples from the aeolian unit (inactive dune, ID; samples Tay 8b-f) (Fig. 6). For the unstratified calcareous silty to sandy samples from the alluvium (inactive gravel sheet, IGS; Tay 8a, Tay 5a-b), a preheat plateau was developed between 240 °C and 260 °C (Fig. 7). Additionally, dose recovery preheat tests for both, alluvial and aeolian samples were carried out. These tests proved that given doses on aeolian and alluvial samples could be reproduced (Figs. 6–8). Finally, we selected a 280 °C preheat temperature and a cut heat of 200 °C for equivalent dose (ED) estimation of the aeolian samples from profile Tay 8. Despite this rather high temperature, thermal transfer did not have any influence on the samples (Fig. 9). For the alluvial samples (Tay 8a, Tay 5a-b), a preheat temperature of 240 °C was chosen.

In contrast to the alluvial sediments in Tay 8a and Tay 5a-b, the aeolian samples showed rather low luminescence sensitivity, although we used 4 mm aliquots containing up to 1500 quartz grains each for all ED measurements (Fig. 5). Recuperation was of minor importance and did not exceed 5% of the natural luminescence signal, which is satisfying. Relatively low luminescence signals were harmful, since a lot of subsamples had to be measured. Frequency distributions of sample Tay 8f and Tay 8a are shown in Fig. 10a-b. ED and dose rate determination (Table 1) resulted in an age of 4900 ± 300 a (Tay 8b) of the sandy infill inside the small ditch and conclusive ages of 5100 ± 400 a (Tay 8c), 4400 ± 300 a (Tay 8d), 3900 ± 200 a (Tay 8e) and 4000 ± 200 a (Tay 8f) for the ID deposit (Table 1, Fig. 11). The five OSL ages are complemented by radiocarbon ages of two charcoal fragments, also collected from the aeolian unit and representing ages of 4190–4420 cal BP (Tay 8/D2 HK) and 3870–4080 cal BP (Tay 8/E2 HK) (Table 2, Fig. 11). The OSL ages of three alluvial samples from the IGS unit below the ancient city wall scatter between 6600 ± 300 a (Tay 8a), 6000 ± 400 a (Tay 5b) and 4900 ± 300 a (Tay 5a) (Table 1, Fig. 11).

5. Discussion

5.1. Luminescence characteristics

To date, little is known concerning luminescence properties of deposits from the northern Arabian Peninsula. The closest study

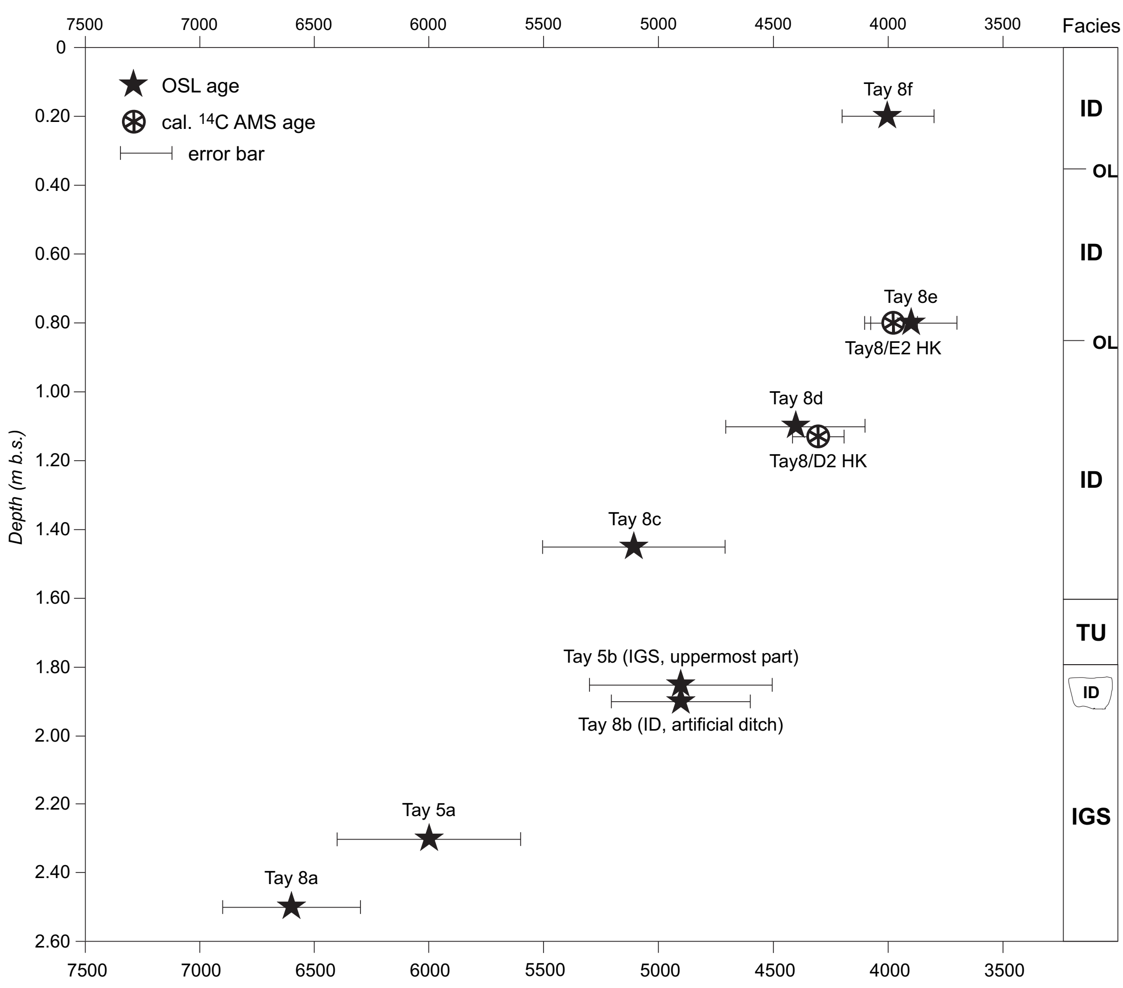

Fig. 11. OSL and ^{14}C ages from profiles Tay 5 and Tay 8 (ID = inactive dune; OL = occupation layer; TU = transitional unit; IGS = alluvium/inactive gravel sheet; BR = bedrock). For more details on the stratigraphy, see Fig. 3.

site is the Al-Quwaiayh area (central Saudia Arabia), where McLaren et al. (2009) report on high luminescence sensitivity of late Pleistocene and Holocene alluvium. However, investigations on aeolian deposits of the Rub al Khali in southern Saudi Arabia (Rosenberg et al., 2009) show that luminescence sensitivity is relatively low. Analogies between distant sites which are most likely of different geological background might appear vague but we observed these properties in our study as well. While the dune sediments showed relatively low luminescence signals, the sensitivity of the alluvial samples at Tayma was clearly higher which is also expressed in considerably higher radionuclide concentrations. X-ray diffraction (XRD) spectra revealed that the inactive gravel sheet (IGS) contains less quartz and higher percentages of feldspar compared to the inactive dune (ID). Calcium carbonate and heavy minerals are even absent in the ID (Fig. 3).

Even though alluvial samples (Tay 8a, Tay 5a-b) from the IGS showed a rather poor preheat plateau, dose recovery preheat tests worked satisfactorily. For the samples from the aeolian unit, both tests confirmed the good applicability of the SAR protocol too. Likewise, resulting luminescence ages from the ID are in stratigraphical order between 3700 and 5500 a (Table 1, Fig. 6) and were validated by the two radiocarbon ages (Table 2, Fig. 11). The luminescence ages of the alluvial samples are in stratigraphic order as well and scatter between 6900 and 4500 a. Although the samples are of alluvial origin, no clear evidence for age overestimation due to partial bleaching was found by means of overdispersion and dose distribution which is Gaussian for sample Tay 8a (Fig. 10).

5.2. Chronological and morphological implications

From a morphodynamic point of view, the ID unit entirely buries the wall section at C1 and OSL ages of its sands represent a minimum age for the construction of the wall, while maximum ages are given by OSL ages of the alluvial samples. Chronological correlation is also given by archaeological investigations that point to a “substantial pre-1st millennium cal BC settlement at Tayma” (Eichmann et al., 2006b, pp. 107) and by waste from early carnelian bead production (5th/4th millennium BC according to Arsebük, 1974, quoted by Eichmann et al., 2006a) which is incorporated into the mud-bricks. The new OSL and ^{14}C data fit this time frame well and provide evidence that the oldest part of the ancient city wall system already existed in the 2nd half of the 3rd millennium BC.

The stratigraphy of profile Tay 8 reveals significant change in morphodynamic processes around 5000 a ago (artificial ditch, Tay 8b in Table 1, 4900 $\pm$ 300 a). The underlying early Holocene IGS implies transport capacities of periodic sheet floods or activation of a mobile wadi network (Vaslet et al., 1994) caused by a more humid climate which is also indicated by a palaeolake in the present sabkha environment north of Tayma (Engel et al., in press) as well as a broad spectrum of palaeoclimatic proxies throughout the Arabian peninsula (e.g. Arz et al., 2003; Fleitmann et al., 2003). To what extent initial settlement activities at Qraya, as indicated by the artificial ditch in profile Tay 8, and subsequent regulation of fluvial dynamics or building measures such as the outer city wall influenced local morphodynamic processes remains subject to future interdisciplinary research. Preliminary results of Hamann et al. (2008) indicate that the outer city wall including the oldest part in excavation square C1 partially served the purpose of regulating wadi channels. The high accumulation rate of the ID indicates that inhabitants were (1) not able or (2) that it was not their intention to prevent the burying of the wall. Only two thin horizons enriched in sherds, snails, edged gravel, bone and charcoal fragments mark temporary stable surfaces at 0.86 m b.s. (c. 4000 a ago according to Tay 8e, Table 1 and Tay 8/E2, Table 2) and 0.35 m b.s. comparable to the desert pavement-like surface covering the ID today.

6. Conclusions

This is the first attempt at optical dating of Holocene deposits from NW Saudi Arabia for the purpose of reconstructing the age of ancient buildings. The aim of the study was to date the construction of the oldest section of the city wall of ancient Tayma. Eight samples for optical dating and two samples for radiocarbon dating were collected from deposits attached to the wall and below its foundations. These deposits were associated with the existence of the wall and therefore, dating its phases of accumulation provides minimum and maximum ages and confines the period of the construction of the wall. Despite low luminescence sensitivity of the aeolian samples OSL measurements were unproblematic and provided conclusive results. Therefore, aeolian samples represent the time when the city wall was erected (minimum age for the construction of the wall). On the other hand, the alluvial sediment which composes the foundation of the city wall gives a maximum age for the construction of the wall. The study shows that dating depositional units which are in clear relative chronological contexts to ancient buildings provide a powerful tool for age determination in the study area. Certainly, optical dating cannot provide the precision of radiocarbon ages or diagnostic artefacts on holocene time scales, but those are not always present, which was the case at the Tayma site. Only two pieces of charcoal were found in the dune sand which were used for independent age control. The conclusive results of OSL and ^{14}C ages suggest the construction of the oldest part of the city wall most likely to the period of the 2nd half of the 3rd mill. BC. More precise evidence cannot be given due to the high errors of the luminescence ages. Further investigations are now concentrated on other, presumably younger parts of the ancient city wall of Tayma to give information about the time of construction.

Acknowledgements

This study was financially supported by the German Research Foundation (DFG) and the Orient Department of the German Archaeological Institute. Logistic support was kindly provided by the Supreme Commission of Tourism of the Kingdom of Saudi Arabia. We thank the referee for constructive comments that helped to improve the manuscript. Andreas Ginau interpreted the XRD-spectra and Kirstin Jacobson helped with language editing.

References

Abu Duruk, H.I., 1986. Introduction to the Archaeology of Tayma. Department of Antiquities and Museums, Riyadh.

Al-Hajri, M., 2006. Brief Preliminary Report on the Excavations at the Industrial Site in Tayma. ATLAL 19, 21–26.

Al-Taimā'i, M.H., 2006. Mintiqa Rujum Sa'sa' Bi-Tayma. Deputy Ministry of Antiquities and Museums, Riyadh.

Arsebük, G., 1974. Addendum: Microlithic assemblage from the Tülintepe Chalcolithic. In: Keban Projekt 1971 Activities. Ankara: Middle East Technical University, Keban Project Publication Series 1 (4), 155–159.

Arz, H.W., Lamy, F., Pätzold, J., Müller, P.J., Prins, M., 2003. Mediterranean moisture source for an early-Holocene humid period in the northern Red Sea. Science 300, 118–121.

Bawden, G., Edens, C., Miller, R., 1980. Preliminary archaeological investigations at Tayma. ATLAL 4, 69–106.

Blechschmidt, I., Matter, A., Preusser, F., Rieke-Zapp, D., 2009. Monsoon triggered formation of Quaternary alluvial megafans in the interior of Oman. Geomorphology 110, 128–139.

Blott, S.J., Pye, K., 2001. Gradistat: a grain size distribution and statistics package for the analysis of unconsolidated sediments. Earth Surf. Proc. Land. 26, 1237–1248.

Bray, H.E., Stokes, S., 2004. Chronologies for Late Quaternary barchan dune reactivation in the southeastern Arabian Peninsula. Quaternary Sci. Rev. 22, 1027–1033.

Doughty, C.M., 1888 (Reprint 2000). Travels in Arabia Deserta, Vol. 1. Adamant Media Corporation, Boston.
Eichmann, R., Schaudig, H., Hausleiter, A., 2006a. Archaeology and epigraphy at Tayma. Arab. Archaeol. Epigr. 17, 163–176.
Eichmann, R., Hausleiter, A, al-Najem, M.H., al-Said, S.F., 2006b. Tayma – Spring 2004, report on the joint Saudi-Arabian–German archaeological project. ATLAL 19, 91–115.
Engel, M., Klasen, N., Ginau, A., Patzke, M., Pint, A., Frenzel, P. and Brückner, H., in press. Palaeoenvironmental change at Tayma (NW Saudi Arabia) as inferred from sabkha infill. In: Eichmann, R., Hausleiter, A. (eds.): Tayma I. Reports on Palaeoenvironment, Archaeology and History. Rahden (Orient-Archäologie).
Euting, J., 1896/1914. Tagebuch einer Reise in Inner-Arabien. Olms, Leiden.
Feathers, J.K., 2003. Use of luminescence dating in archaeology. Meas. Sci. Technol. 14, 1493–1509.
Fleitmann, D., Burns, S.J., Mudelsee, M., Neff, U., Kramers, J., Mangini, A., Matter, A., 2003. Holocene forcing of the Indian monsoon recorded in a stalagmite from Southern Oman. Science 300, 1737–1739.
Fuchs, M., Woda, C., Bürkert, A., 2007. Chronostratigraphy of a sediment record from the Hajar mountain range in north Oman: implications for optical dating of insufficiently bleached sediments. Quat. Geochronol. 2, 202–207.
Galbraith, R.F., Roberts, R.G., Laslett, G.M., Yoshida, H., Olley, J.M., 1999. Optical dating of single grains of quartz from Jinmium rock shelter, northern Australia. Part I: experimental design and statistical models. Archaeometry 41, 339–364.
Glennie, K.W., Singhvi, A.K., 2002. Event stratigraphy, paleoenvironment and chronology of SE Arabian deserts. Quaternary Sci. Rev. 21, 853–869.
Goudie, A.S., Colls, A., Stokes, S., Parker, A., White, K., Al-Farraj, A., 2000. Latest Pleistocene and Holocene dune construction at the north-eastern edge of the Rub Al Khali, United Arab Emirates. Sedimentology 47, 1011–1021.
Hamann, M., Heemeier, B., Patzelt, A., Grottker, M., 2008. Wasserwirtschaftliche Anlagen in der historischen Oasenstadt Tayma, Saudi-Arabien. In: Ohlig, C. (Ed.), Cura Aquarum in Jordanien. Schriften der DWhG 12, 155–175.
Hausleiter, A., 2010. Excavations in the large representative building E-b1 and its surroundings. In: Eichmann, R., Hausleiter, A., al-Najem, M.H., al-Said, S.F. (Eds.), Tayma – Autumn 2004 and Spring 2005, 2nd Report on the Joint Saudi-Arabian-German Archaeological Project. ATLAL 20, 101–147.
Intilia, A., 2010. Area C. In: Eichmann, R., Hausleiter, A., al-Najem, M.H., al-Said, S.F. (Eds.), Tayma – Autumn 2004 and Spring 2005, 2nd Report on the Joint Saudi-Arabian-German Archaeological Project. ATLAL 20, 101–147.
Köhn, M., 1928. Bemerkungen zur mechanischen Bodenanalyse. III. Ein neuer Pipettierapparat. J. Plant Nutr. Soil Sci. 11, 50–54.
Kulig, G., 2005, Erstellung einer Auswertesoftware zur Altersbestimmung mittels Lumineszenzverfahren unter spezieller Berücksichtigung des Einflusses radioaktiver Ungleichgewichte in der 238U-Zerfallsreihe. Unpublished BSc thesis, Technical University, Bergakademie Freiberg.
Livingstone, A., Spaie, B., Ibrahim, M., Kamal, M., Taimani, S., 1983. Taima: Recent Soundings and New Inscribed Material (1402/1982). ATLAL 7, 102–116.
McLaren, S., Al-Juaidi, F., Bateman, M.D., Millington, A.C., 2009. First evidence for episodic events in the arid interior of central Saudi Arabia over the last 60 ka. J. Quaternary Sci. 24 (2), 198–207.
Murray, A.S., Wintle, A.G., 2000. Luminescence dating of quartz using an improved single aliquot regenerative-dose protocol. Radiat. Meas. 32, 57–73.
Parr, P., Harding, G.L., Dayton, J.E., 1970. Preliminary Survey in N.W. Arabia, 1968. Bull. Inst. Archaeol., Univ. London 8–9, 193–242.
Philby, H.S.J., 1957. The Land of Midian. Benn, London.
Preusser, F., 2009. Chronology of the impact of Quaternary climate change on continental environments in the Arabian Peninsula. C. R. Geosci. 341, 621–632.
Preusser, F., Radies, D., Matter, A., 2002. 160 ka record of dune development in Southern Arabia and atmospheric circulation patterns. Science 296, 2018–2020.
Reimer, P.J., Baillie, M.G.L., Bard, E., Bayliss, A., Beck, J.W., Blackwell, P.G., Bronk Ramsey, C., Buck, C.E., Burr, G.S., Edwards, R.L., Friedrich, M., Grootes, P.M., Guilderson, T.P., Hajdas, I., Heaton, T.J., Hogg, A.G., Hughen, K.A., Kaiser, K.F., Kromer, B., McCormac, F.G., Manning, S.W., Reimer, R.W., Richards, D.A., Southon, J.R., Talamo, S., Turney, C.S.M., van der Plicht, J., Weyhenmeyer, C.E., 2009. IntCal09 and Marine09 radiocarbon age calibration curves, 0–50,000 years cal BP. Radiocarbon 51, 1111–1150.
Rhodes, E.J., Bailey, R.M., 1997. The effect of thermal transfer on the zeroing of the luminescence of quartz from recent glaciofluvial sediments. Quaternary Sci. Rev. 16, 291–298.
Rosenberg, T., Preusser, F., Fleitmann, D., 2009. Aeolian quartz from Saudi Arabia with OSL-ages to beyond the Eemian. First results from a paleoclimate study on lakebeds. In: UK Luminescence and ESR Meeting. Dept. of Geography, Royal Holloway University of London, August 2009 (Abstract Volume).
Schneider, P., 2010. Mauern in Tayma. In: Lorenzen, J., Pirson, F., Schneider, P., Wulf-Rheidt, U. (Eds.), Aktuelle Forschungen zur Konstruktion, Funktion und Semantik antiker Stadtbefestigungen. Byzas 10, 1–25.
Stokes, S., Bray, S.E., 2005. Late Pleistocene aeolian history of the Liwa region. Arabian Peninsula. Geol. Soc. Am. Bull. 117, 1466–1480.
Vaslet, D., Janjou, D., Robelin, C., Al Muallem, M.S., Halawani, M.A., Brosse, J.M., Breton, J.P., Courbouleix, S., Roobol, M.J., Dagain, J., 1994. Explanatory Notes to the Geologic Map of the Tayma Quadrangle, Sheet 27C, Kingdom of Saudi Arabia, Scale 1:250,000. Directorate General of Mineral Resources, Jiddah.
Wellbrock, K., Grottker, M., 2010. Reconstruction of Mid-Holocene Climate Conditions for North-Western Arabian Oasis Tayma. Proceedings of the 4th International Conference on Water Resources and Arid Environments, 5-8 December 2010, Riyadh, Saudi Arabia, 694–703.
Whitney, J., Faulkender, W., Rubin, M., 1983. The Environmental History and Present Condition of Saudi Arabia's Northern Sand Seas. USGS Open-File Report, 83–749.
Winnett, F.V., Reed, W.L., 1970. Ancient Records from North Arabia. Toronto University Press, Toronto/Buffalo.
Wintle, A.G., 2008. Fifty years of luminescence dating. Archaeometry 50 (2), 276–312.
Zander, A., Degering, D., Preusser, F., Kasper, H.U., Brückner, H., 2007. Optically stimulated luminescence dating of sublittoral and intertidal sediments from Dubai, UAE: Radioactive disequilibria in the uranium decay series. Quat. Geochronol. 2, 123–128.